Electrochemical Route for the Synthesis of New Nanostructured Magnetic Mixed Oxides of Mn, Zn, and Fe from an Acidic Chloride and Nitrate Medium

F. Torres, R. Amigó, J. Asenjo, E. Krotenko, and J. Tejada

Departament de Física Fonamental, Facultat de Física, Universitat de Barcelona, Diagonal 647, 08028 Barcelona, Spain

E. Brillas*

Laboratori de Ciència i Tecnologia Electroquímica de Materials, Departament de Química Física, Facultat de Química, Universitat de Barcelona, Diagonal 647, 08028 Barcelona, Spain

Received March 20, 2000. Revised Manuscript Received July 3, 2000

New nanostructured magnetic Mn−Zn−Fe oxides are electrochemically synthesized as precipitates from chloride + nitrate solutions of pH 1.5 with Mn^{2+}, Zn^{2+}, and Fe^{2+}, or Fe^{3+} at temperatures between 40 and 80 °C using electrodes of commercial iron. The process has been studied using an undivided cell of 100 mL and a stirring batch tank of 700 mL with electrodes of 20 and 140 cm^2 area, respectively. Fe^{2+} is continuously supplied to the solution from oxidation of the sacrificial Fe anode, although this ion can be transformed into Fe^{3+} by reaction with Mn^{3+}, previously formed by anodic oxidation of Mn^{2+}. An energy cost of ca. 5 kWh kg^{-1} is found for the batch tank at 35 mA cm^{-2}. For solutions up to 30 mM Mn^{2+} and 15 mM Zn^{2+}, magnetic precipitates richer in Fe than in Zn and Mn, with Cu impurity proceeding from the anode, are obtained. These materials have an inverse cubic spinel structure, being composed of nanoparticles formed by solid solutions of iwakiite, franklinite, magnetite, and maghemite. Magnetically, they behave as soft ferrites but show lower initial permeability. In contrast, superparamagnetic nanoparticles are synthesized by electrolyzing solutions with 110−120 mM Mn^{2+} and 30 mM Zn^{2+}. These materials with more Mn than Zn and Fe are formed by amorphous mixed oxide, along with two different crystalline phases composed of hetaerolite and a mixture of iwakiite and franklinite, respectively.

I. Introduction

Mn−Zn−Fe oxides are magnetic compounds widely used in core materials for inductors and transformer devices in telecommunication applications, magnetic recording, audio and video devices, and so on. These ferrites combine interesting soft magnetic properties with relatively high electrical resistivity that permits low eddy−current losses in ac applications.[1,2] Commercial Mn−Zn−Fe oxides are composed of particles of micrometric size with a spinel crystalline structure and are traditionally produced by combination of MnO−ZnO−Fe_2O_3 mixtures at high temperature (ca. 1000 °C), following a long and expensive procedure involving powder preparation, shaping, firing, and finishing.[1−3] The chemical composition and microstructure of ferrites thus obtained affect strongly their physical properties. Recently, new Mn−Zn−Fe oxides with very high initial permeability ($\mu_i \geq 20\,000$) have been prepared from the above conventional procedure.[4] Alternative methods to produce these compounds can give rise to new materials with other interesting technological applications.

In the past few years, there has been great interest in the synthesis and characterization of nanostructured materials with particle sizes from 1 to 100 nm.[5−20] The fascinating electronic, optical, and magnetic properties

* Telephone: (34) 93 4021223. Fax: (34) 93 4021231. E-mail: e.brillas@qf.ub.es.

(1) Kirk-Othmer. *Encyclopedia of Chemical Technology*, 4th ed.; John Wiley & Sons: New York, 1993; Vol. 10, pp 383−384.
(2) Cahn, R. W., Ed. *The Encyclopedia of Advanced Materials*; Pergamon: New York, 1994; Vol. 2, pp 800−803.
(3) ASM Handbook Committee. *Metal Handbook*, 9th ed; American Society for Metals: Ohio, 1980; Vol. 3, p 606.
(4) Lucke, R. *J. Phys. IV France* **1998**, *8*, Pr2−437.
(5) Inskeep, W. P. J. *Environ. Qual.* **1989**, *18*, 379.
(6) Dormann, J.; Fiorani, D. *Magnetic Properties of Fine Particles*; North-Holland: Amsterdam, 1992.
(7) Ziolo, R. F.; Giannelis, E. P.; Weinstein, B. A.; O'Horo, M. P.; Ganguly, B. N.; Mehrotra, V.; Russel, M. W.; Huffman, D. R. *Science* **1992**, *257*, 219.
(8) Nixon, L.; Koval, C. A.; Noble, R. D. *Chem. Mater.* **1992**, *4*, 1770.
(9) Matijevic, E. *Chem. Mater.* **1993**, *5*, 412.
(10) Odenbach, S. *Adv. Colloid Interface Sci.* **1993**, *46*, 263.
(11) Cao, H.; Suib, S. L. *J. Am. Chem. Soc.* **1994**, *116*, 5334.
(12) Suryanarayana, C. *Int. Mater. Rev.* **1995**, *40*, 41.
(13) Leslie-Pelecky, D.; Rieke, R. D. *Chem. Mater.* **1996**, *8*, 1770.
(14) Reetz, M. T.; Helbig, W.; Quasier, S. A. In *Active Metals: Preparation, Characterization, Applications*; Fürstner, A., Ed.; VCH: Weinheim, 1996.
(15) Tejada, J.; Ziolo, R. F.; Zhang, X. X. *Chem. Mater.* **1996**, *8*, 1784.
(16) Mounien, N.; Pileni, M. P. *Chem. Mater.* **1996**, *8*, 1128.
(17) Cao, X.; Koltypin, Y.; Prozorov, R.; Kataby, G.; Gedanken, A. J. *Mater. Chem.* **1997**, *7*, 2447.
(18) Grimm, S.; Schultz, M.; Barth, S.; Müller, R. I. *Mater. Sci.* **1997**, *32*, 1083.
(19) Pascal, C.; Pascal, J. L.; Favier, F.; Elidrisi-Moubtassim, M. L.; Payen, C. *Chem. Mater.* **1999**, *11*, 141.
(20) Amigó, R.; Asenjo, J.; Krotenko, E.; Torres, F.; Tejada, J.; Brillas, E. *Chem. Mater.* **2000**, *12*, 573.

10.1021/cm001043h CCC: $19.00
Published on Web 09/23/2000

of nanoparticles are attractive prospects for information storage, bioprocessing, color imaging, magnetic refrigeration, ferrofluids, and gas sensors. Among these compounds, nanostructured metal oxides can be obtained from different chemical methods involving oxidation in micellar media or in polymer or mineral matrixes,[16] oxyhydrogen flame pyrolysis,[18] and sol−gel processes.[5] An alternative electrochemical route has also been reported by Pascal et al.[19] for the generation of amorphous and magnetic nanoparticles of maghemite (γ-Fe_2O_3) with sizes between 3 and 8 nm using a sacrificial iron anode in an organic medium with cationic surfactants as stabilizer.

Recently, we have proposed[20] a low-cost electrochemical procedure for the synthesis of magnetic mixed oxides of Sr and Fe. It consists of the electrolysis of a solution with Sr^{2+} and Fe^{3+} at constant current density using two Fe electrodes. Thus, soluble Fe^{2+} is continuously supplied to the electrolyte from the two-electron oxidation of the sacrificial Fe anode:

$$Fe \rightarrow Fe^{2+} + 2e^- \quad (1)$$

whereas the main cathodic reaction corresponds to water reduction to H_2 gas:

$$2H_2O + 2e^- \rightarrow H_2 + 2OH^- \quad (2)$$

New magnetic Sr−Fe oxide nanoparticles with a crystalline structure similar to that of maghemite and magnetite (Fe_3O_4) are collected as precipitates from nitrate or chloride solutions between 20 and 90 °C with energy costs of ca. 4 kWh kg^{-1}. To explain the formation of such mixed oxides, maghemite and magnetite are assumed to be produced in the alkaline region near the cathode from eqs 3 and 4, respectively. The resulting mixture of these oxides is further doped by Sr^{2+}, which partially substitutes the Fe^{2+} of magnetite to yield the final insoluble Sr−Fe oxide. This process is shown in eq 5, where *a*/*b* represents the stoichiometric proportion of the maghemite/magnetite mixture doped by one Sr^{2+}.

$$2Fe^{3+} + 6OH^- \rightarrow \gamma\text{-}Fe_2O_3 + 3H_2O \quad (3)$$

$$Fe^{2+} + 2Fe^{3+} + 8OH^- \rightarrow Fe_3O_4 + 4H_2O \quad (4)$$

$$Sr^{2+} + [(\gamma\text{-}Fe_2O_3)_a(Fe_3O_4)_b] \rightarrow [(\gamma\text{-}Fe_2O_3)_a(Fe_3O_4)_{b-1}(SrFe_2O_4)] + Fe^{2+} \quad (5)$$

Sr−Fe oxides with high Sr contents and a coercitivity up to 8 kA m^{-1} are thus generated from chloride media in the pH range 1−12, although they have a small amount of metallic Fe (<5% in weight) impurities formed by reduction of electrogenerated Fe^{2+}. In nitrate media, metallic Fe is not detected, but the Sr content in precipitates is so low that nonmagnetic materials are found at pH > 3. These results suggest that the use of acidic chloride + nitrate media can be more suitable to produce large proportions of nanostructured magnetic mixed oxides, avoiding the formation of Fe impurities.

Following the above-proposed electrochemical method, we have undertaken a study trying to synthesize new nanostructured magnetic Mn−Zn−Fe oxides by electrolyzing solutions of pH 1.5 with chlorides and nitrates of Mn^{2+}, Zn^{2+}, and Fe^{3+} or Fe^{2+}. Commercial iron has been chosen as electrodic material for both the sacrificial anode and the cathode to achieve a cheap process, suitable to be industrialized. The electrolytic experiments have been performed in an undivided cell of 100 mL and a stirring batch tank of 700 mL at different salt compositions, current densities, and temperatures. The composition, microstructure, and magnetic properties of mixed oxides collected as precipitates in all chloride + nitrate solutions have been determined by inductively coupled plasma (ICP), energy-dispersive X-ray spectrometry (EDX), scanning electron microscopy (SEM), X-ray diffraction (XRD), and SQUID magnetometry. The results obtained in this study are reported herein.

II. Experimental Section

The mixed oxides were synthesized from electrolytes containing mixtures of ferrous chloride tetrahydrate, ferric chloride hexahydrate, manganous chloride tetrahydrate, manganous nitrate tetrahydrate, zinc chloride, and zinc nitrate hexahydrate. All of these salts were analytical or puriss. grade from Panreac and Merck. Analytical grade hydrochloric acid supplied by Panreac was used to regulate the solution pH. All electrolytic solutions were prepared with bidistilled water.

Electrolyses were performed with Hewlett-Packard 6643A and 6554A dc power supplies. The solution pH was measured with a Crison 2002 pH meter. XRD spectra of mixed oxides collected in solution were recorded on a Siemens D-500 Bragg−Brentano $\theta/2\theta$ geometry powder diffractometer at the wavelength of the Kα band for Cu ($\lambda = 1.5418$ Å). Their morphology was examined by SEM with a Leica LC 360 scanning electron microscope. The composition of the single particles obtained was determined by EDX with a JEOL JSM840 scanning electron microscopy. The composition in weight of the commercial iron used as electrode was analyzed by inductively coupled plasma-mass spectrometry (ICP-MS) with a Perkin-Elmer Elan 6000 spectroscope. The Mn, Zn, Fe, and Cu contents in the mixed oxides were obtained by ICP using a Jobin Yvon JY38VHR inductively coupled argon plasma spectroscope. The saturation magnetization M_s, remanent magnetization M_r, and coercive field H_c for each precipitate were recorded on a Quantum Design MPMS5.5 SQUID magnetometer. The same instrument was employed to measure its zero-field-cooled and field-cooled curves.

Experiments were conducted in two different undivided cells with commercial iron electrodes as both the anode and the cathode. Iron electrodes were polished before use to eliminate surface oxides. Their average composition was determined by ICP-MS: Fe, 99.5%; Mn, 0.4%; Cu, 0.1%. Some electrolyses were performed with a one-compartment cylindrical cell of 100 mL capacity having a jacket to be thermostated with an external circuit of water. The anode and the cathode of this cell were foils of 50 × 40 × 3 mm in dimension with 20 cm^2 of area immersed in the solution and separated by ca. 4 cm. The electrolytic solution was stirred with a magnetic bar. Other trials were carried out with a batch tank of 120 × 120 × 80 mm in dimension and 700 mL capacity. The electrodes employed were plates of 110 × 100 × 3 mm in dimension, which were suspended in parallel into the reactor at a distance of ca. 2 cm with 140 cm^2 of area immersed in the solution. The electrolyte bulk was mechanically stirred with a PTFE-coated steel shaft coupled to a Heidolph RZR1 stirrer. In some cases, the batch tank was immersed in a water bath to be thermostated during the trial.

Solutions containing different concentrations of Fe^{2+}, Fe^{3+}, Mn^{2+}, and Zn^{2+} in chloride + nitrate media were acidified with concentrated HCl to pH 1.5 and further electrolyzed by applying a constant current density *j*. The cell voltage *V* was directly read on power supplies. The solution pH was adjusted to its initial value every 15 min by adding small volumes of HCl. The temperature was maintained within the range

Table 1. Weights and Energy Costs for Magnetic Mixed Oxides Obtained from Electrolysis of Solutions of pH 1.5 with *u* mM $FeCl_2$ + *v* mM $FeCl_3$ + *w* mM $MnCl_2$ + *x* mM $Mn(NO_3)_2$ + *y* mM $ZnCl_2$ + *z* mM $Zn(NO_3)_2$ under Different Experimental Conditions

	solution[a]											
expt	*u* mM	*v* mM	*w* mM	*x* mM	*y* mM	*z* mM	*T* °C	*j* [b] mA cm^{-2}	*V*[c] V	*t*[d] *h*	oxide wt[e] g	energy cost kWh kg^{-1}
Cell of 100 mL												
1	10	5	7.5	7.5	7.5	7.5	60	100	6.4	3	5.03	7.6
2	10	5	7.5	7.5	7.5	7.5	40	250	14.4	3	13.07	16.5
3	10	5	15	15	5		40	250	14.5	3	14.73	14.8
Batch Tank of 700 mL												
4	10	5	15	15	7		40	35	4.5	5	22.08	5.1
5	1		10	10	6	6	80	35	4.3	4.5	20.63	4.7
6	1		15	15	10		49[f]	43	5.7	5	36.65	4.7
7	1		60	60	30		51[f]	65	7.5	1.5	5.45	18.6
8			60	50	30		55[f]	57	6.8	2.5	31.16	4.3

[a] The solution pH was adjusted to its initial value every 15 min. [b] Applied current density. [c] Average cell voltage. [d] Electrolysis time. [e] Overall magnetic mixed oxide weight collected from the solution, the cathode, and the anode. [f] Average temperature reached by the nonthermostated solution.

between 40 and 80 °C. In all cases, large amounts of magnetic mixed oxides were produced. The major part of these materials precipitate in solution, although smaller amounts of oxides were also collected at the cathode and, in much less proportion, at the anode. After every electrolysis, the magnetic precipitate suspended in solution was directly extracted with a permanent $Nd_2Fe_{14}B$ magnet. The products retained at the anode and cathode were previously separated by washing with bidistilled water, and further, their magnetic components were extracted with the permanent magnet. Each magnetic mixed oxide obtained was rinsed with bidistilled water, diluted HCl, and bidistilled water again to eliminate all soluble salts, being finally dried in an oven at 80 °C until constant weight. The energy cost for each process was determined as the consumed kilowatt-hour per kilogram of total collected magnetic precipitate.

III. Results and Discussion

In a first attempt to produce magnetic Mn−Zn−Fe oxides, a series of experiments was carried out using the cell of 100 mL with a background electrolyte containing a mixture of $FeCl_2$, $FeCl_3$, $MnCl_2$, $Mn(NO_3)_2$, $ZnCl_2$, or $Zn(NO_3)_2$. Fe^{2+} was initially added to the electrolyte to ensure the formation of magnetite close to the cathode by eq 4 from the beginning of the electrolysis. The entrance flow of Fe^{2+} to the solution was further regulated by operating at different constant *j* values ranging between 100 and 250 mA cm^{-2}. The solution pH was adjusted to 1.5 and the temperature was kept at 40 and at 60 °C. Results obtained for several trials (expts 1−3) are summarized in Table 1. An increase in energy cost of magnetic precipitate from 7.6 to ca. 16 kWh kg^{-1} can be observed with increasing current density from 100 to 250 mA cm^{-2}, practically independent of salt composition. This trend is mainly accounted for by the increase in cell voltage due to the higher ohmic drop (current × resistance product) of solution, because ca. 2.5 times more of magnetic oxide weight are produced. In all cases, about 75% of the final dry precipitates was magnetic. Most of these products were collected in solution (45−50%), and lower proportions were obtained from the cathode (22−25%) and anode (<4%). It is noteworthy that a fast increase in solution pH took place during all electrolyses, owing to the continuous production of OH^- at the cathode from eq 2. A part of such OH^- ions is consumed in the formation of magnetic and nonmagnetic oxides near the cathode (see, for example, eqs 3 and 4).

Table 2. Magnetic Properties at 300 K, Average Particle Size, and Stoichiometry as $MnZn_iFe_jO_k$ (with Cu impurity) Determined by ICP for Mixed Oxides Recovered as Precipitates in Solution and Electrochemically Synthesized under the Conditions Reported in Table 1

						stoichiometry			
expt	M_s kA m^{-1}	M_r kA m^{-1}	H_c kA m^{-1}	μ_i[a]	*d*[b] nm	*i*	*j*	*k*[c]	*l*[d]
1	66	7.4	3.1	18	21.8	3.5	22	38	1×10^{-3}
2	87	6.6	4.1	18	22.3	1.8	106	162	5×10^{-3}
3	58	9.1	5.4	18	18.3	0.8	28	48	9×10^{-3}
4	69	11	3.4	29	19.4	2.2	22	37	2×10^{-3}
5	78	13	4.5	24	21.3	3.7	25	41	4×10^{-3}
6	69	14	5.8	49	22.1	1.9	16	24	3×10^{-3}
7[e]		0.03	2.1	1	23.2	0.6	0.4	2.2	$<1 \times 10^{-4}$
8[e]		0.005	0.16	1	25.3	0.9	1.0	4.5	6×10^{-4}

[a] Initial permeability determined from the slope of the *M*−*H* linear plot at low *H* values (<20 kA m^{-1}). [b] Estimated by applying the Scherrer equation to the maximum peak of the corresponding XRD spectrum related to an inverse cubic spinel structure. [c] Calculated from the difference between the weight of the mixed oxide sample and the weight of metals contained in it. [d] Cu/Mn ratio. [e] In expts 7 and 8, superparamagnetic particles were produced.

The electrochemical synthesis of Mn−Zn−Fe oxides was confirmed by ICP analysis of magnetic precipitates collected in solution from expts 1 to 3. The resulting average formulas expressed as $MnZn_iFe_jO_k$ are given in Table 2. As can be seen, ternary oxides show a very variable stoichiometry with predominance of Fe over Mn and Zn, and an O/Fe ratio ranging between 1.5 and 1.8. The material richer in Zn is obtained in expt 1, with formula $MnZn_{3.5}Fe_{22}O_{38}$ and an O/Fe ratio of 1.73. These findings suggest the existence of complex pathways for the generation of Mn−Zn−Fe oxides in which the complexant power of Cl^- and NO_3^- with metallic ions and intermediates plays an important role in the extension of reactions involved. In addition, a Cu content of <1% of Mn (see Table 2) is also present in these precipitates. This impurity proceeds from the oxidation of metallic Cu contained in the anode to yield Cu^{2+}, which is further incorporated to the magnetic precipitate.

To corroborate the electrochemical synthesis of mixed oxides, the composition of single particles collected in solution was analyzed by EDX. A spectrum for the sample of expt 1 is shown in Figure 1. Strong Kα and Kβ bands for Mn, Fe, and Zn, along with a weaker Kα

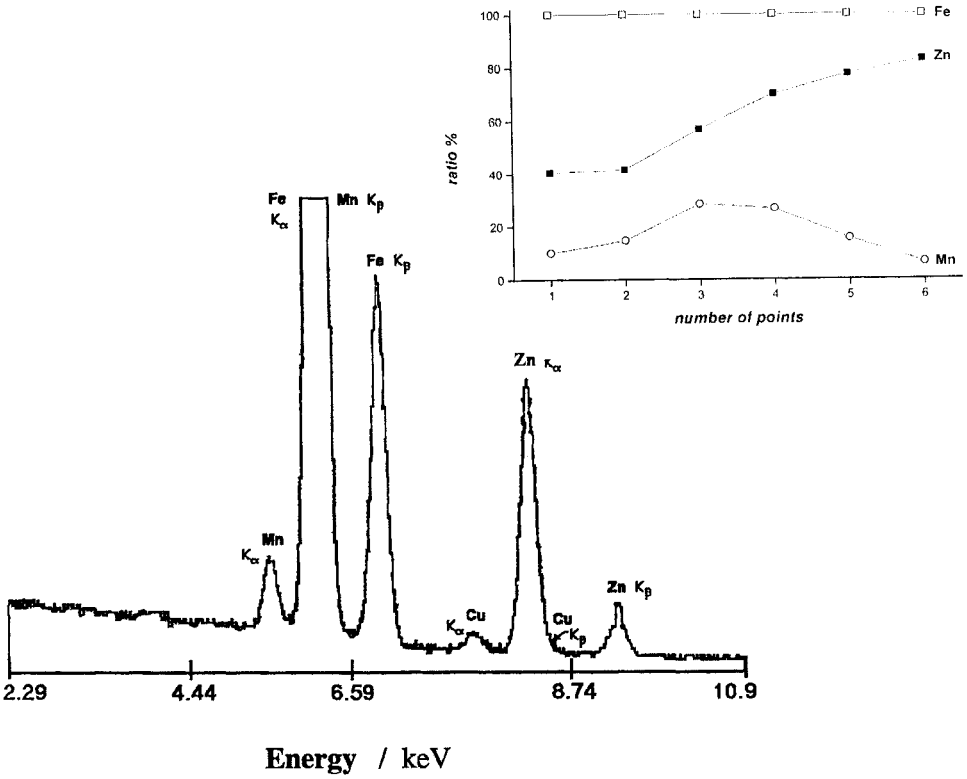

Figure 1. EDX spectrum of single particles of the magnetic mixed oxide collected as precipitate in solution from expt 1. The relative ratio between Fe, Mn, and Zn in percentage for different points of the sample with a spot size of about 1.5 μm is given as inset.

band for Cu, can be observed, indicating that particles are composed of ternary oxides of Mn, Zn, and Fe, with Cu impurities. Its homogeneity was examined by recording EDX spectra at different points of the sample. The calculated spot size[21] was ca. 1.5 μm. The relative ratio between Fe, Zn, and Mn for each point was estimated from the corresponding area of pure Kα bands for Zn and Mn with respect to that of the pure Kβ band for Fe, assumed as 100%. The results obtained, given in Figure 1, show a variable composition of Fe, Mn, and Zn very far from a homogeneous phase of mixed oxides. This confirms the complexity of processes involved in their generation, in agreement with ICP results of Table 2. On the other hand, SEM images of these materials reveal that they are formed by nanoparticles with size <50 nm.

The XRD spectrum recorded for the Mn−Zn−Fe oxides precipitated in solution from expt 1 is presented in Figure 2. Similar peaks are found for the magnetic oxides obtained in expts 2 and 3. All of these crystalline materials have an inverse cubic spinel structure intermediate to that of franklinite ($ZnFe_2O_4$), magnetite, and maghemite, as can be seen in the magnification of the maximum peak at ca. 35° in the 2θ scale shown in Figure 2. Their spectra are also similar to that of iwakiite ($MnFe_2O_4$), which crystallizes in the tetragonal system with practically equal lattice constants of a = 8.519 Å and c = 8.540 Å. It is noteworthy that peaks associated with chlorides or nitrates of Mn^{2+}, Zn^{2+}, Fe^{2+}, and Fe^{3+} are not observed, because all of these salts are eliminated when rinsing the precipitates with diluted HCl and water. In addition, peaks related to metallic Fe are not detected, such as previously found in the Sr−Fe oxides obtained in chloride medium.[20] This fact indicates an inhibition of the cathodic reduction of Fe^{2+} to Fe by nitrate ions present in the electrolyte.

The above XRD results allow one to calculate the lattice constant a for the inverse cubic spinel structure of the biggest crystals formed by Mn−Zn−Fe oxides. For example, a = 8.431 ± 0.002 Å is determined for the precipitate obtained in expt 1, a value very close to that of franklinite (a = 8.441 Å), magnetite (a = 8.396 Å), and maghemite (a = 8.351 Å). The average particle size d for synthesized mixed oxides was also estimated from their XRD spectra applying the Scherrer equation in the form $d = 0.94\,\lambda/L\cos\theta$, where λ is the wavelength of the Kα band for Cu and L is the full width in radians at the half-height of the maximum intensity peak at a 2θ angle of ca. 35°. The d values thus obtained are in the nanometric scale, being lower than 23 nm (see Table 2).

Once it confirmed that the proposed electrochemical method is useful to prepare magnetic Mn−Zn−Fe oxides, the study was extended to the batch tank of 700 mL to clarify the effect of salt concentration on their generation process. A first trial (expt 4) was performed in this system at 35 mA cm^{-2} for 5 h and at 40 °C using a salt composition similar to that of the cell of 100 mL. A lower energy cost of ca. 5 kWh kg^{-1} is found for the magnetic precipitate recovered in the batch tank due to the lower density current and cell voltage applied (see Table 1). The formula $MnZn_{2.2}Fe_{22}O_{37}$, EDX spectra and SEM images of single particles, XRD spectrum, and d = 19.4 nm determined for the material collected in solution from expt 4 are quite similar to those obtained

(21) Goldtein, J. I.; Newbury, D. E.; Echlin, P.; Joy, D. C.; Fiori, C.; Lifshin, E. *Scanning Electron Microscopy and X-ray Microanalysis*; Plenum Press: New York, 1984.

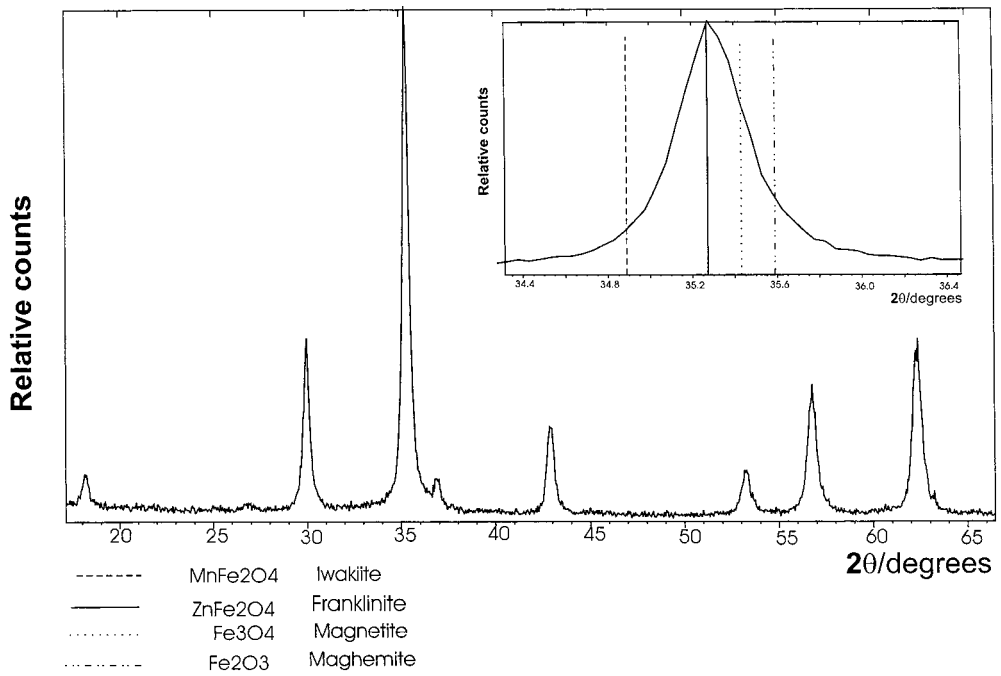

Figure 2. XRD spectrum corresponding to the sample of Figure 1. At the top right-hand part, a magnification of the maximum peak at ca. 35° in the 2θ scale.

in expts 1−3 (see Table 2). These findings indicate that the process can easily be scaled working under similar experimental conditions.

Further experiments in the batch tank were carried out starting from electrolytes either with only 1 mM $FeCl_2$ or in the absence of Fe^{2+} and Fe^{3+} ions. Two kind of chloride + nitrate solutions were tested, one of them containing up to 30 mM Mn^{2+} and 15 mM Zn^{2+} (expts 5 and 6), and the other one with higher concentrations of 110−120 mM Mn^{2+} and 30 mM Zn^{2+} (expts 7 and 8). As can be seen in Table 1, all of these trials are effected at current densities between 35 and 65 mA cm^{-2} with temperatures between 50 and 80 °C and yield magnetic precipitates. The energy cost for most of these electrolyses ranges between 4.3 and 4.7 kWh kg^{-1}. For expt 7, however, a higher consumption of 18.6 kWh kg^{-1} is found, because of the production of a smaller amount of magnetic precipitate. It is noteworthy that in expts 7 and 8 an increasing layer of oxides grew in the cathode causing a gradual increase in cell voltage, the reason for which they were stopped after 1.5 and 2.5 h of electrolysis, respectively.

ICP, EDX, SEM, and XRD analyses of precipitates collected in solution from expts 5 and 6 give results similar to those described above for expts 1−4 (see Table 2). In contrast, a very different behavior is observed for magnetic oxides recovered from expts 7 and 8. Results of Table 2 show that their average formula is $MnZn_{0.6}Fe_{0.4}O_{2.2}$ and $MnZn_{0.9}Fe_{1.0}O_{2.2}$, respectively, i.e.; the content in Mn is higher than that of Zn and Fe, and the O/Fe ratio varies between 4.5 and 5.5. In both materials, Cu is practically undetected as an impurity (<0.06% of Mn). EDX spectra of their single particles confirm the formation of high-purity Mn−Zn−Fe oxides, and SEM analysis indicates the formation of nanoparticles with size < 50 nm. Their XRD spectra (see Figure 3) show the coprecipitation of a large proportion of amorphous material and two different crystalline phases with tetragonal and inverse cubic spinel structures. The lattice constants for the minority tetragonal crystals are $a = 5.742 \pm 0.002$ Å and $c = 9.149 \pm 0.002$ Å, in good agreement with $a = 5.720$ Å and $c = 9.245$ Å for hetaerolite ($ZnMn_2O_4$). For the majority inverse cubic spinel crystals, the lattice constant is $a = 8.380 \pm 0.002$ Å, and their XRD peaks are quite similar to those of iwakiite and franklinite. The average particle size determined from this last structure is ca. 25 nm, as can be seen in Table 2 for expts 7 and 8.

The above results indicate the generation of new nanostructured magnetic Mn−Zn−Fe oxides, not described previously in the literature, by the proposed electrochemical route using chloride + nitrate solutions of pH 1.5. These materials, however, are also produced starting from electrolytes without Fe^{3+} ions (expts 5−8), and then, a part of Fe^{2+} produced from eq 1 is transformed into Fe^{3+} under our experimental conditions. This process cannot be due to the direct oxidation of Fe^{2+}, because Fe^{3+} is not formed by electro-dissolution of an Fe anode.[20] Since Mn^{2+} present in the starting solution is an ion easily oxidable in acidic medium, one can consider that it can be oxidized to Mn^{3+} at the Fe anode:

$$Mn^{2+} \rightarrow Mn^{3+} + e^- \qquad (6)$$

Mn^{3+} can then react in the vicinity of the anode with Fe^{2+} to give Fe^{3+} with Mn^{2+} regeneration:

$$Fe^{2+} + Mn^{3+} \rightarrow Fe^{3+} + Mn^{2+} \qquad (7)$$

Thus, the presence of Fe^{3+} in the electrolyte under our experimental conditions can be accounted for by the production of Mn^{3+} as catalytic intermediate.

Experimental results for solutions up to 30 mM Mn^{2+} and 15 mM Zn^{2+} (expts 1−6) indicate that materials present a higher content in Fe than in Mn and Zn, with an O/Fe ratio between 1.5 and 1.8, suggesting that they are formed by solid solutions of mixtures of maghemite

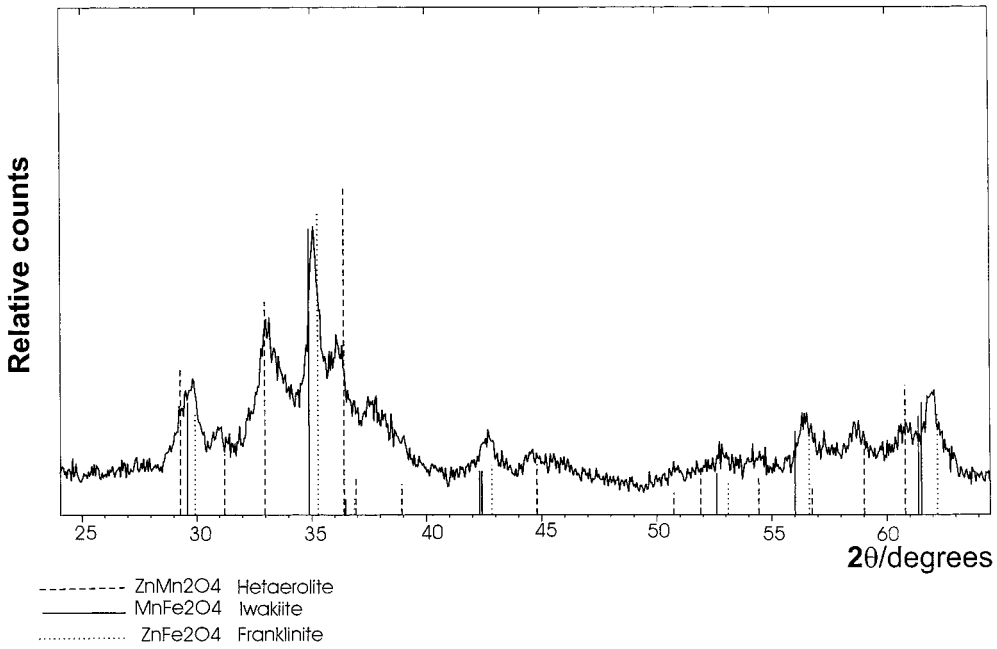

Figure 3. XRD spectrum obtained for the magnetic Mn−Zn−Fe oxide collected as precipitate in solution from expt 8.

with O/Fe ratio = 1.50, magnetite with O/Fe ratio = 1.33, and magnetite doped with Mn^{2+} (iwakiite) and Zn^{2+} (franklinite), both with O/Fe ratio = 2.00. Maghemite and magnetite can be produced in the vicinity of the cathode from eqs 3 and 4, respectively. The applied electric field between electrodes promotes the further partial substitution of Fe^{2+} of magnetite by Mn^{2+} and Zn^{2+}, leading to the final insoluble mixed oxide:

$$Mn^{2+} + iZn^{2+} + [(\gamma\text{-}Fe_2O_3)_a(Fe_3O_4)_b] \rightarrow [(\gamma\text{-}Fe_2O_3)_a(Fe_3O_4)_{b-i-1}(MnFe_2O_4)(ZnFe_2O_4)_i] + (i+1)Fe^{2+} \quad (8)$$

The final compound can be expressed in the form $MnZn_iFe_jO_k$ with $j = 2a + 3b - i - 1$ and $k = 3a + 4b$. The fact that i varies between 0.8 and 3.7 (see Table 2) indicates that Zn^{2+} has higher doping power than Mn^{2+}. The presence of Cu impurity in such oxides can be ascribed to the coprecipitation of $CuFe_2O_4$, formed by doping of magnetite with Cu^{2+} obtained by oxidation of metallic Cu of the anode. In contrast, solutions containing 110−120 mM Mn^{2+} and 30 mM Zn^{2+} (expts 7 and 8) yield a mixture of unidentified amorphous material and two crystalline phases, where Mn predominates over Zn and Fe. The majority crystals with inverse cubic spinel structure can then be related to a mixture of iwakiite and franklinite, whereas the minority tetragonal crystals are due to the coprecipitation of hetaerolite.

The magnetic properties of all Mn−Zn−Fe oxides determined by SQUID magnetometry are also listed in Table 2. As can be seen, the behavior of samples of expts 1−6 is very different from those of expts 7 and 8. This can easily be deduced by comparing the hysteresis cycles recorded for samples of expts 1 (Figure 4a) and 8 (Figure 4b). While the $M-H$ plot for the former mixed oxide shows a maximum magnetization of 66 kA m^{-1}, the second one behaves as a superparamagnetic material without reaching the saturation of magnetization until fields of 800 kA m^{-1}. Results of Table 2 show that all

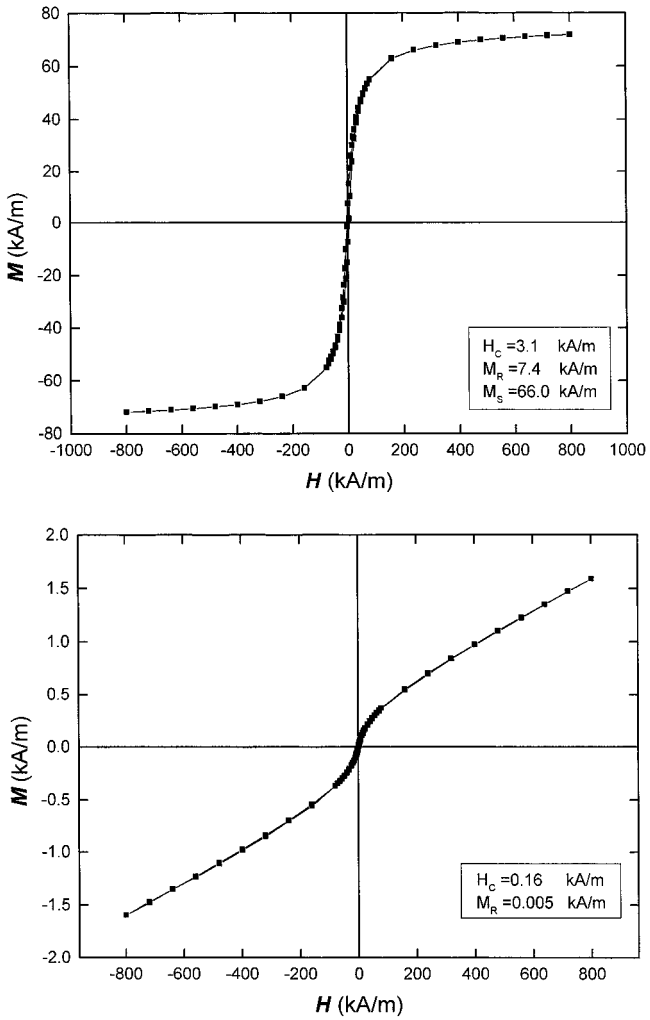

Figure 4. Magnetic characterization at 300 K of the Mn−Zn−Fe oxide collected in solution from expts (a) 1 and (b) 8.

samples of expts 1−6 have magnetic characteristics of soft ferrites with saturation and remanent magnetizations lower than 87 and 14 kA m^{-1}, respectively, and

coercive fields lower than 6 kA m^{-1}. The fact that these mixed oxides are formed by nanoparticles can explain[22] their low initial permeability ($\mu_i < 50$) in comparison with the value of ca. 20 000 found for the best samples of microstructured Mn−Zn−Fe oxides prepared from the traditional high-temperature method.[4] A suitable post-treatment including thermal and rotating magnetic field processes has then to be developed to increase the initial permeability and magnetic properties of nanoparticles of Mn−Zn−Fe oxides obtained by the proposed electrochemical route. It is noteworthy that such generated materials can directly be utilized for the same applications as those ordinary commercial soft ferrites with $\mu_i < 100$, because they show similar magnetic characteristics, having the advantage of their much lower production cost.

To gain a better understanding of the magnetic behavior of synthesized mixed oxides, their zero-field-cooled and field-cooled curves were recorded. The procedure[15,23] consists of cooling the sample to 10 K in zero field, then a $H = 16$ kA m^{-1} is applied, and the sample is slowly heated to 300 K while measuring the change in magnetization with temperature. This is the so-called zero-field-cooled magnetization, M_{ZFC}. Once the temperature of 300 K is reached, the sample is cooled again to 10 K while maintaining the external magnetic field of 16 kA m^{-1}, and the variation of magnetization with temperature is subsequently recorded until 300 K. This dependence corresponds to the field-cooled magnetization, M_{FC}. The analysis of both, $M_{ZFC}(T)$ and $M_{FC}(T)$ curves allows one to determine the following: (*i*) the blocking temperature T_b, i.e., the temperature at which $M_{ZFC}(T)$ reaches its maximum value; (*ii*) the irreversibility temperature where the $M_{ZFC}(T)$ and $M_{FC}(T)$ curves split, associated with the interaction between the particles. Thus, at temperatures smaller than T_b, the magnetic moment of most of the particles is "blocked", whereas at $T > T_b$, the particles are superparamagnetic.[23]

The zero-field-cooled and field-cooled curves for magnetic Mn−Zn−Fe oxides obtained in expts 4 and 8 are presented in parts a and b, respectively, of Figure 5. As can be seen, only in Figure 5b do both curves show a maximum at T_b ca. 50 K, overlapping above 175 K. The precipitate of expt 8 should then be superparamagnetic at $T > 50$ K, such as experimentally found at room temperature. However, the T_b value for the mixed oxides collected in solution from expts 1−6 is higher than 300 K, as in the case shown in Figure 5a for the sample of expt 4. Consequently, these materials behave as soft ferrites at room temperature.

IV. Conclusions

It has been demonstrated that new nanostructured magnetic Mn−Zn−Fe oxides are obtained as precipitates by electrolyzing an acidic medium with chloride and nitrates of Mn^{2+}, Zn^{2+}, and Fe^{2+} or Fe^{3+} using commercial iron electrodes. Fe^{2+} is continuously supplied to the solution from oxidation of the sacrificial Fe anode, although this ion can partially be transformed into Fe^{3+} by reaction with Mn^{3+}, previously formed by anodic oxidation of Mn^{2+}. The process can easily be scaled from an undivided cell of 100 mL to a stirring batch tank of 700 mL. In this last system, the energy cost for magnetic materials collected is as low as 5 kWh kg^{-1}. Two kind of magnetic mixed oxides with different composition, structure, and magnetic properties can be synthesized from the proposed electrochemical method depending on salt concentration. For solutions up to 30 mM Mn^{2+} and 15 mM Zn^{2+}, precipitates richer in Fe than in Zn and Mn are obtained in solution, although they have a very small proportion of Cu impurities proceeding from the oxidation of metallic Cu contained in the anode. These materials of high crystallinity have an inverse cubic spinel structure, being composed of nanoparticles with solid solutions of iwakiite, franklinite, magnetite, and maghemite. The two last compounds are formed from eqs 3 and 4, respectively, whereas iwakiite and franklinite are produced by further doping of magnetite with Mn^{2+} and Zn^{2+}, respectively, under the action of the applied electrical field in the vicinity of the cathode. All collected samples show magnetic properties such as typical soft ferrites at room temperature, with $M_s \leq 87$ kA m^{-1}, $M_r \leq 14$ kA m^{-1}, and $H_c < 6$ kA m^{-1}. In contrast, electrolyses of solutions with 110−120 mM Mn^{2+} and 30 mM Zn^{2+} lead to the synthesis of superparamagnetic nanoparticles at room temperature. These materials are deposited on the cathode causing a progressive increase in cell voltage.

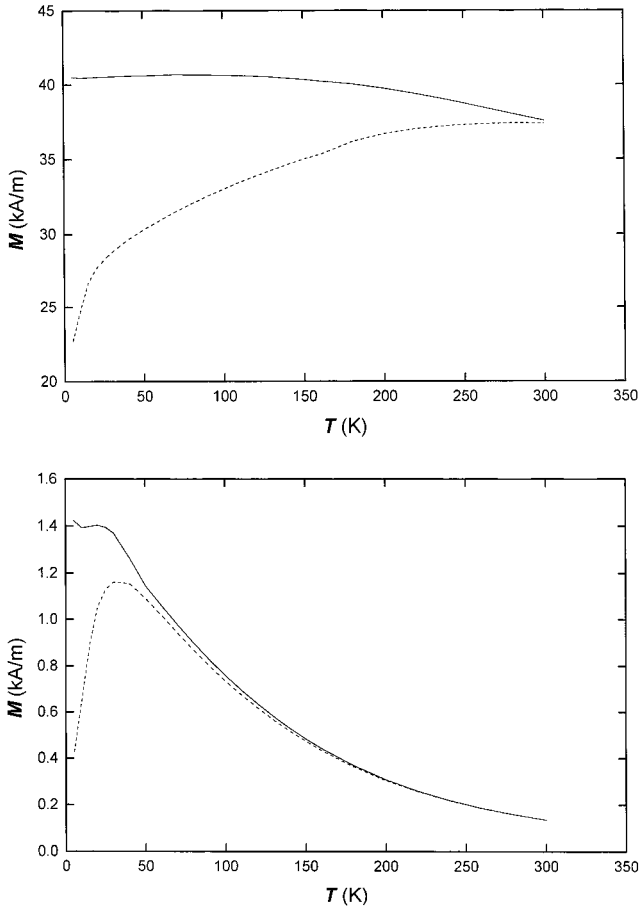

Figure 5. (- - -) Zero-field-cooled and (−) field-cooled curves recorded at $H = 16$ kA m^{-1} for the Mn−Zn−Fe oxide obtained in solution from expts (a) 4 and (b) 8.

(22) Jiles, D. *Introduction to Magnetism and Magnetic Materials*; Chapman and Hall: New York, 1992.

(23) Chudnovsky, E. M.; Tejada, J. *Macroscopic Quantum Tunneling of the Magnetic Moment*; Cambridge University Press: Cambridge, 1998.

The precipitates in solution contain more Mn than Zn and Fe, and their XRD spectra indicate the presence of a large proportion of amorphous mixed oxide, along with two crystalline phases with inverse cubic spinel and tetragonal structures. The first crystals correspond to a mixture of iwakiite and franklinite, whereas the second ones are due to the coprecipitation of hetaerolite. The zero-field-cooled and field-cooled curves recorded for these precipitates indicate that they behave as superparamagnetic materials from 50 K.

Acknowledgment. The authors thank the European Community for financial support received for this work under Brite-EuRam III Project BRST-CT98-5267 and are grateful to the "Serveis-Científico Tècnics" of the Universitat de Barcelona for its help in analyses of magnetic mixed oxides.

CM001043H